Combustion and Flame 190 (2018) 74–86

Contents lists available at ScienceDirect

Combustion and Flame

journal homepage: www.elsevier.com/locate/combustflame

Probing the low-temperature chemistry of ethanol via the addition of dimethyl ether

Yingjia Zhang[a,b], Hilal El-Merhubi[c], Benoîte Lefort[c], Luis Le Moyne[c], Henry J. Curran[b], Alan Kéromnès[c,*]

[a] State Key Laboratory of Multiphase Flow in Power Engineering, Xi'an Jiaotong University, Xi'an 710049, China
[b] Combustion Chemistry Centre, National University of Ireland, Galway, Ireland
[c] DRIVE EA1859, Université Bourgogne Franche Comté, F58000 Nevers, France

ARTICLE INFO

Article history:
Received 24 August 2017
Revised 15 October 2017
Accepted 10 November 2017
Available online 28 November 2017

Keywords:
Ignition delay times
Ethanol
DME
Low-temperature chemistry

ABSTRACT

Considering the importance of ethanol (EtOH) as an engine fuel and a key component of surrogate fuels, the further understanding of its auto-ignition and oxidation characteristics at engine-relevant conditions (high pressures and low temperatures) is still necessary. However, it remains difficult to measure ignition delay times for ethanol at temperatures below 850 K with currently available facilities including shock tube and rapid compression machine due to its low reactivity. Considering the success of our recent study of toluene oxidation under similar conditions [38], dimethyl ether (DME) has been selected as a radical initiator to explore the low-temperature reactivity of ethanol. In this study, ignition delay times of ethanol/DME/'air' mixtures with blending ratios of 100% EtOH, 70%/30% EtOH/DME and 50%/50% EtOH/DME mixtures were measured in a rapid compression machine and in two high-pressure shock tubes at conditions relevant to internal combustion engines (20–40 atm, 650–1250 K and equivalences ratios of 0.5–2.0). The influence of these conditions on the auto-ignition behavior of the mixture blends was systematically investigated. Our results indicate that, in the low temperature range (650–950 K), increasing the amount of DME in the fuel mixture significantly increases the reactivity of ethanol. At higher temperatures, however, there is almost no visible impact of the fuel mixture composition, whereas DME shows a lower reactivity. Furthermore, with the addition of DME, different kinetic regimes were observed experimentally: the reactivity is controlled by ethanol when the addition of DME is less than 30% while it is dominated by DME when the proportion of DME is over 50%. Literature mechanisms show reasonable agreement with the new experimental data for the 100% EtOH and the 70%/30% EtOH/DME mixtures but under-predict the reactivity of the 50%/50% EtOH/DME mixtures at temperatures below 850 K, suggesting that further refinement of the low-temperature chemistry of ethanol/DME is warranted. An updated binary fuel mechanism is therefore proposed by incorporating the latest experimental and/or theoretical work in the literature, as well as adding new reaction pathways. Results indicate that the proposed model is in satisfactory agreement with all of the mixtures investigated.

1. Introduction

Ethanol and DME are considered to be promising transportation biofuels due to their sustainability [1–5] and low soot emissions [6–8] in internal combustion engines (ICEs). In order to determine its potential use in real internal combustion engines, it is important to investigate a priori how it will behave under practical engine relevant conditions. Ethanol also has an impact on the reactivity of surrogate fuels. Compared to mixtures made of primary reference fuels (PRF), *n*-heptane and iso-octane, ternary mixtures including ethanol present a reduced negative temperature coefficient (NTC) behavior at low temperature at a constant octane number. The reactivity is reduced at low temperatures (below 750 K) but increases at intermediate and high temperatures [9]. Thus, ethanol has previously been extensively studied under various range of conditions and facilities including flame speed measurements [10–16], ignition delay times measurements in shock tube [17–21] and rapid compression machines [21–23], species measurements in rapid compression facility [23], flow reactors [9,24–26] and jet-stirred reactors [27]. There is, however, limited experimental data with which to evaluate the auto-ignition behavior of ethanol under engine relevant conditions, namely at high

* Corresponding author.
E-mail address: alan.keromnes@u-bourgogne.fr (A. Kéromnès).

https://doi.org/10.1016/j.combustflame.2017.11.011
0010-2180/

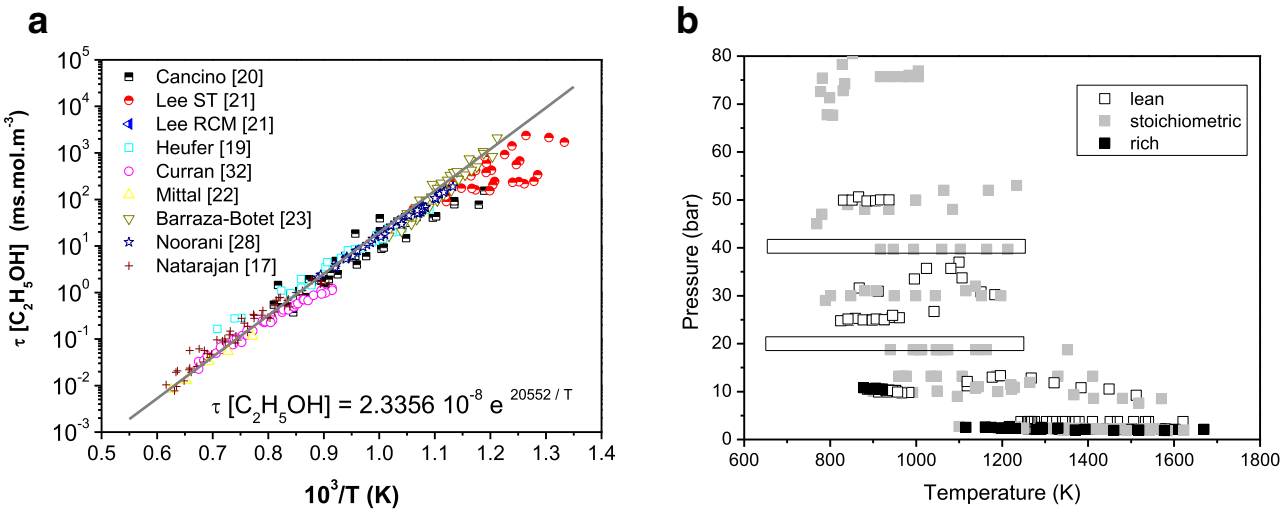

Fig. 1. Comparison of the available ignition delay time data (symbols) [17,19–23,28,32] with the experimental conditions presented in this study (boxes).

pressures and at intermediate to low temperatures (especially below 850 K) [22], since most of the experimental investigation has been performed at low pressure (below 5 bar) and at high temperatures (above 1000 K). Considering measurements performed at high pressures, Heufer and Olivier [19] measured the ignition delay times of the stoichiometric ethanol–air mixture at 13, 19 and 40 bar in the temperature range of 910–1410 K using a shock tube. Cancino et al. [20] investigated the ignition for lean ethanol–air mixture ($\varphi = 0.3$) at 30 bar between 860 K and 1180 K and for stoichiometric mixture over a pressure range of 10–50 bar with a temperature range of 800–1250 K in a shock tube. Lee et al. [21] performed a shock tube and RCM study of stoichiometric ethanol–air mixture under high pressure conditions (67–93 bar) in the intermediate temperature range (775–1000 K). Mittal et al. [22] investigated the auto-ignition behavior of lean ethanol–air mixture ($\varphi = 0.3$ and 0.5) in the intermediate temperature range (830–980 K) for a pressure range of 10–50 bar and of stoichiometric mixture at 10 bar and over limited temperature range (870–920 K). More recently, Barraza-Botet et al. [23] measured ignition delay times and species concentration for a diluted stoichiometric ethanol/O_2 mixture in a rapid compression facility at temperature between 880 and 1120 K over a pressure range of 3–10 bar. Extended experimental work on ethanol ignition, including lean to rich mixtures, has been mainly performed at intermediate and high temperatures (>850 K), low pressures (≤10 atm) and at diluted conditions in shock tubes [17,28,29]. The available data are summarized in Fig. 1b. It appears that there is a lack of data at low temperatures (<850 K) and at high pressures (>10 atm). This lack of data limits the construction, validation and interpretation of chemical kinetic mechanism for the real combustor design. Such data are particularly important in assessing the influence of blending ethanol with practical fuels, in which the low reactivity of ethanol will inhibit the reactivity of a fuel at these low temperature conditions [30,31]. Moreover, Mittal et al. [22] revealed some discrepancies in the data available at low temperature (<910 K) whereas there is a very good agreement at high temperature (>910 K). However, some scatter appears at lower temperatures. The ignition delay times measured by Lee et al. [21] are shorter than expected. In their paper, Lee et al. scrutinized the ignition phenomenon using Schlieren imaging. They notice inhomogeneous ignition events with the occurrence of ignition kernels, leading to a pre-ignition pressure rise and associated pressure rise prior to ignition. Thus, the experiments cannot be considered as being at constant volume conditions. In order to use these peculiar data for kinetic model validation, Lee et al. indicated that these non-ideal facility effects should be taken into account. Moreover, in RCMs, in the low temperature range, ignition delay times are slightly longer than expected as these are affected by heat transfer to the walls which lowers the temperature inside the combustion chamber and reduces the reactivity of the system.

Therefore, it is crucial to scrutinize the auto-ignition of ethanol at this low to intermediate temperature regime and provide reliable data in order to accurately predict the reactivity of ethanol which are of interest for internal combustion engine operation. The goal of the present study is to answer to this need and provide a comprehensive set of ignition delay times over a broad temperature range for fuel-lean to fuel-rich conditions and at high pressure.

The recent study from Barraza-Botet et al. [23] suggests that the accuracy of rate constants for ethanol + $H\dot{O}_2$ needs to be improved. This was confirmed by Olm et al. [33] who performed an optimization of an ethanol mechanism previously published by Saxena and Williams [15]. This also calls into question our understanding of the low temperature chemistry of ethanol.

Detailed chemical kinetics mechanisms have been proposed by several authors [11,15,20,21,25,27,34–36]. Dunphy et al. [34] validated a kinetic mechanism against ignition delay time measurements performed at low pressures (2–4.5 bar) and at high temperatures (1100–1500 K). Egolfopoulos et al. [11] proposed a mechanism tested under low pressure conditions (1 bar) including ignition delay times, species profiles measured in a flow reactor and laminar flame speeds. Marinov [35] validated his mechanism against a wide range of experimental conditions including laminar flame speeds, species profiles measured in a jet-stirred reactor and flow reactor and ignition delay times. Li et al. [25] studied the decomposition of ethanol in a flow reactor and proposed a rate constant for the decomposition reaction $C_2H_5OH = C_2H_4 + H_2O$ in order to improve the mechanism previously developed by Marinov. Saxena and Williams [15] proposed a new mechanism validated at low pressures (1–4 bar) against flame speeds, ignition delay times and species profiles. Cancino et al. [20] built their mechanism based on that of Marinov and validated it against ignition delay times at high pressure conditions (10–50 bar) for fuel-lean and stoichiometric mixtures. Leplat et al. [27] derived their mechanism by combining the mechanism developed by Marinov [35] and GRI Mech [36].. They increased the pressure range to 10 bar by testing the mechanisms against species data measured in a jet-stirred reactor and flame speeds and reproduced these data with good agree-

ment. Lee et al. [21] revisited the mechanism proposed by Li et al. [25] and extended the validation to high pressures (80 bar) based on ignition delay time measurements performed in a high-pressure shock tube and in a rapid compression machine for stoichiometric ethanol–air mixtures. Metcalfe et al. [37] proposed a C_1–C_2 mechanism validated against a wide range of conditions including ethanol combustion targets.

In the present study, ignition delay times have been measured in a rapid compression machine and in shock tubes covering fuel-lean to fuel-rich conditions ($\varphi = 0.5$, 1.0 and 2.0) over a wide range of temperature (650–1250 K) at pressures relevant to internal combustion engines (20 and 40 bar). However, due to the limitations of our experimental facilities (especially heat transfer), it is difficult to measure long ignition delay times (>300 ms) at temperatures below 825 K, conditions which are relevant to ethanol–air mixtures. Recently, in order to probe its low temperature chemistry, toluene was blended with dimethyl ether in order to test a mechanism's ability to reproduce accurately the reactivity of various binary mixture combinations [38]. Due to the success of that study, DME has again been selected as a radical initiator to test the predictive capability of a mechanism to accurately reproduce the experimentally observed reactivity of binary ethanol/DME mixtures and extend the measurable temperature range to 650 K. In order to assess the inhibiting effect of ethanol, different blending ratios have been tested: ethanol/DME: 0/100, 50/50, 30/70, 100/0. Using this experimental database, the chemical kinetic mechanism has been revised and its performance has been evaluated against these binary mixtures and data available in the literature.

In the following sections, the experimental devices are described, followed by a presentation and a discussion of the experimental results. Then, the revised chemical kinetic mechanism is presented and its performance in reproducing experimental results is discussed.

2. Experimental devices

The experiments were carried out in a rapid compression machine (RCM) at NUI Galway and two high-pressure shock tubes (NUI Galway and DRIVE). Ignition delay times of ethanol/DME/'air' mixtures were measured at conditions relevant to those encountered in ICEs (pressure: 20–40 bar, temperature: 650–1250 K, equivalence ratio: 0.5–2.0, and blending ratio: ethanol/DME: 0/100, 50/50, 30/70, 100/0 in 'air'). All mixtures were prepared manometrically in heated stainless-steel tanks. The partial pressure of ethanol was maintained below one third of its vapor pressure in order to avoid any condensation of the fuels in the tanks. Moreover, all of the intake manifolds, the RCM, and the two HPSTs were heated for the same purpose. The ethanol used in this study was obtained from Sigma-Aldrich at 99.5+% purity and O_2, N_2 and He were supplied by BOC Ireland and Air Liquide at 99.5%, 99.95% and 99.9%, respectively.

The RCM is a horizontally-opposed twin-piston device that has been described previously [39,40]. The symmetry of the RCM allows a short adiabatic compression process (16–17 ms) and helps to reduce the aerodynamic effects inside the combustion chamber at the end of the compression process [41]. Moreover, the piston heads include a crevice which captures the vortex created by the piston corner compression. Thus, the mixture and the temperature are homogeneous prior to ignition. The pressures and temperatures achieved at the end of the compression process (P_C and T_C respectively) in this study were 20 and 40 bar and 650–1050 K, respectively. The final conditions were reached by changing the initial pressure and temperature. For all experiments, the pressure and the position of both pistons are recorded using a digital oscilloscope. The pressure profile recorded with a pressure transducer (Kistler 601A) provided the compression time and was used to measure the ignition delay time. It was defined as the time difference between the end of the compression process and the maximum rate of pressure increase. The temperature, T_C, is calculated using the initial temperature, T_i, and pressure, P_i, and the compressed gas pressure, P_C, assuming adiabatic compression and frozen chemistry and using Gaseq [42]. For each experimental condition an experiment with a non-reactive mixture was performed by replacing oxygen with nitrogen in the test mixture since they have similar thermodynamic properties. The recorded pressure profile is used in order to take into account heat losses when simulating the experiments. A heating system controlled by five thermocouples is used to heat five different positions, namely the left and right collar, the left and right sleeve and the reaction chamber on the RCM. The T_i can be adjusted from 30 to 120 °C with a maximum 5 °C temperature unevenness (at temperature of 120 °C), which can cause 10–15 °C uncertainty in the T_C estimated using the following equation:

$$\ln\left(\frac{p_c}{p_i}\right) = \int_{T_i}^{T_c} \frac{\gamma}{\gamma - 1}\frac{dT}{T} \tag{1}$$

In addition, the P_i and P_C monitored by pressure transmitter (MKS TYPE 121) and pressure transducer (Kistler 601A) as well as heat capacity (γ) of the prepared combustible mixture can also cause a minor uncertainty in the T_C. In general, the uncertainty in T_C is estimated to be ±20 K [43,44].

The experiments at DRIVE were carried out in a high-pressure shock tube which has been described previously [45]. The stainless-steel tube has an inner diameter of 50 mm and is divided by a double membrane (stainless-steel diaphragm) into two sections (a driver section of 4 m and a driven section of 5 m) constituting a small section called "intermediate section (IS)". In addition of the main tube, this facility includes a vacuum system (a roughing pump and a turbo-molecular pump) which evacuated the tube and the stainless-steel tanks to pressures below 5 Pa, a velocity detection system (based on four individual piezoelectric pressure transducers PCB 113B22) and a data acquisition system (NI Compact RIO). The tube, mixing tanks and manifold were preheated to 80 °C to avoid any condensation of ethanol by ensuring its partial pressure is below one third of its vapor pressure. Post-shock pressures, P_5, are measured using a Kistler piezoelectric pressure transducer (603B1) located at the endwall. The temperature, T_5, behind the reflected shock wave is calculated using the shock wave velocity in conjunction with the 1-D shock relations and the species thermodynamics using the chemical equilibrium software Gaseq [42] with an accuracy of ±1% which corresponds to ±10–15 K according to the uncertainty calculation proposed by Petersen et al. [46]. The Kistler pressure transducer is also used to determine the qualitative, transient pressure and to determine the ignition delay time. It is defined as the time interval between the time when the pressure and temperature conditions behind the reflected shock wave are reached and the onset of combustion, commonly defined by sudden change in pressure.

In order to cross-check the reliability of the data recorded in both facilities ignition delay times of the ethanol/air mixture at 20 and 40 atm at $\varphi = 1.0$ were measured in the NUI Galway HPST, described previously [47]. Briefly, the HPST has a constant inner diameter of 63.5 mm with a 3.0 m driver section and a 5.7 m driven section. Two pre-scored aluminium diaphragms were used to control the bursting pressure and to promote an ideal bursting of the diaphragm with a uniform petaling which minimizes undesirable fluid dynamics during incident shock formation. The tube, mixing tank and manifold were pre-heated to 75 °C to allow the partial pressure of ethanol in the prepared mixture be four times lower than its vapor pressure. The mixtures so prepared were allowed to diffusively mix for 12 h before performing experiments. The endwall pressures, monitored by a Kistler 603B pressure transducer,

Table 1
Mixtures investigated in this study.

Equivalence ratio (φ)	DME (%)	Ethanol (%)	O_2 (%)	N_2 (%)	Device
0.5	–	3.38	20.29	76.33	NUIG RCM & ST + DRIVE ST
	1.01	2.37	20.29	76.33	NUIG RCM + DRIVE ST
	1.69	1.69	20.29	76.33	NUIG RCM + DRIVE ST
	3.38	–	20.29	76.33	NUIG RCM & ST
1.0	–	6.54	19.63	73.83	NUIG RCM + DRIVE ST
	1.96	4.58	19.63	73.83	NUIG RCM + DRIVE ST
	3.27	3.27	19.63	73.83	NUIG RCM + DRIVE ST
	6.54	–	19.63	73.83	NUIG RCM + DRIVE ST
2.0	–	12.28	18.42	69.30	NUIG RCM + DRIVE ST
	3.68	8.60	18.42	69.30	NUIG RCM + DRIVE ST
	6.14	6.14	18.42	69.30	NUIG RCM + DRIVE ST
	12.28	–	18.42	69.30	NUIG RCM + DRIVE ST

were used to identify the ignition delay times. The reflected shock conditions were calculated using Gaseq [42] with input of the measured incident shock velocity determined by six PCB 113B24 pressure transduces. The largest uncertainties presented here were estimated to be ±15% for ignition delay times and ±20 K in reflected shock temperatures according to the calculation proposed by Petersen et al. [46].

All mixtures were tested in the RCM in order to measure the ignition delay times in the low temperature range. For the experiments at higher temperatures, they were performed in the DRIVE high-pressure shock tube, except for the mixtures without ethanol which were previously measured at NUIG [48]. However, in order to complete the database, ignition delay times of DME were measured in DRIVE at 40 bar for mixtures of $\varphi = 1$ and 2. Moreover, the experiments without DME were measured in both shock tubes to allow the comparison of experimental results and showed good agreement. The test matrix is detailed in Table 1.

3. Update of chemical kinetic mechanism

The base mechanism used in the current study is taken from AramcoMech 1.3, which includes the $H_2/CO/O_2$ sub-mechanism developed by Kéromnès et al. [49] and the C_1–C_2 sub-mechanism established by Metcalfe et al. [37]. The sub-mechanisms of ethanol and DME are adopted from the recent work of Mittal et al. [22] and Burke et al. [48] respectively, in which AramcoMech 1.3 was used as the base mechanism. The thermochemistry is taken from AramcoMech 1.3 and thermodynamic parameters of new species are estimated using the group additivity method employed by Zellner and Benson [50] and implemented in THERM [51]. In order to take into account facility effects, mainly heat losses to the walls, when simulating the RCM, variable volume–time profiles were used [52]. Generally, the original model predicts our new data at high temperatures whereas it does not agree well with the new ignition delay time data measured in this study, Fig. 2. Particularly for the 50%/50% EtOH/DME mixtures at temperatures below 770 K, the mechanisms predict a greater reactivity and ignition delay times that are between 10% and 20% shorter than the experimental results.

This suggests that further improvement of the model for binary EtOH/DME fuel mixtures is warranted. The important reactions controlling both ethanol and DME oxidation chemistry are highlighted in the "brute-force" sensitivity analysis, Fig. 3, and will be discussed here. The sensitivity coefficient calculated (S) is determined using Eq. (2):

$$S = \frac{\ln(\tau_+/\tau_-)}{\ln(k_+/k_-)} = \frac{\ln(\tau_+/\tau_-)}{\ln(2.0/0.5)} \quad (2)$$

where $\tau+$ and $\tau-$ are the computed ignition delay times corresponding to respectively, an increase and decrease by a factor of two in a rate coefficient (k). A negative sensitivity coefficient corresponds to an increase in reactivity (a decrease in ignition delay time with an increase in rate constant).

3.1. Hydrogen atom abstraction

For the 100% EtOH system, H-atom abstraction by $H\dot{O}_2$ radicals at the alpha site on ethanol shows the highest promoting effect on ignition delay times. Unfortunately, neither experimental measurements nor theoretical calculations of this rate constant are available in the literature. Metcalfe et al. [37] made an analogical analysis of the reaction of n-butanol with $H\dot{O}_2$ radicals calculated by Zhou et al. [53] to simulate the shock tube data and showed good agreement with the experimental measurements. However, in the subsequent study of Mittal et al. [22] it was pointed out that using the rate constant recommended by Metcalfe et al. [37] underpredicted their measured RCM ignition delay times, and thus the rate constant of this reaction was modified to better predict the reactivity of ethanol at lower temperatures. Nevertheless, Mittal's model is still not capable of predicting well the ignition delay times at the relatively high pressures (75 bar) measured by Lee et al. [21]. With this in mind, we re-optimized the Arrhenius parameters based on Mittal's recommendation [22]. Specifically, the rate constant for H-atom abstraction by $H\dot{O}_2$ radicals from the alpha site has been increased by reducing both the A-factor by 15% and the activation energy by 0.7 kcal mol^{-1}. The adjusted rate constant is 1.8 and 0.94 times higher than the upper limit calculated by Zhou et al. [53] at 800 K and 1800 K, respectively. Moreover, the rate constants for abstraction from the beta and $\dot{O}H$ sites remain the same as those calculated by Zhou et al. [53]. Figure 4 shows the effect on the high-pressure reactivity of ethanol of adopting Mittal's rate for the reaction $C_2H_5OH + H\dot{O}_2 = CH_3\dot{C}HOH + H_2O_2$. Clearly, the addition of the Mittal et al. recommendation causes a significant over-prediction of ignition delay times when compares to the modified value utilized in the proposed model.

It should be noted that the reactivity of the 100% EtOH mixture is not particularly sensitive to H-atom abstraction from ethanol by $\dot{O}H$ radicals. However, H-atom abstraction at the alpha site shows the strongest inhibiting effect and the overall promotion in reactivity is more prominent in the presence of DME due to the higher concentrations of $\dot{O}H$ radicals generated from the low temperature chain-branching processes involved in DME oxidation. This observation is similar to our recent study of toluene/DME ignition [38]. The rate constant used by Mittal et al. was originally taken from Sivaramakrishnan et al. [54], but the authors increased the A-factor by 25% and maintained the total rate of $\dot{O}H$ consumption via H-atom abstraction from ethanol. This adjustment leads to approximately 28% of the branching ratio for abstraction at the beta site. Recently, Stranic et al. [55] measured the total rate constant and branching ratio for the reaction at the beta site behind reflected

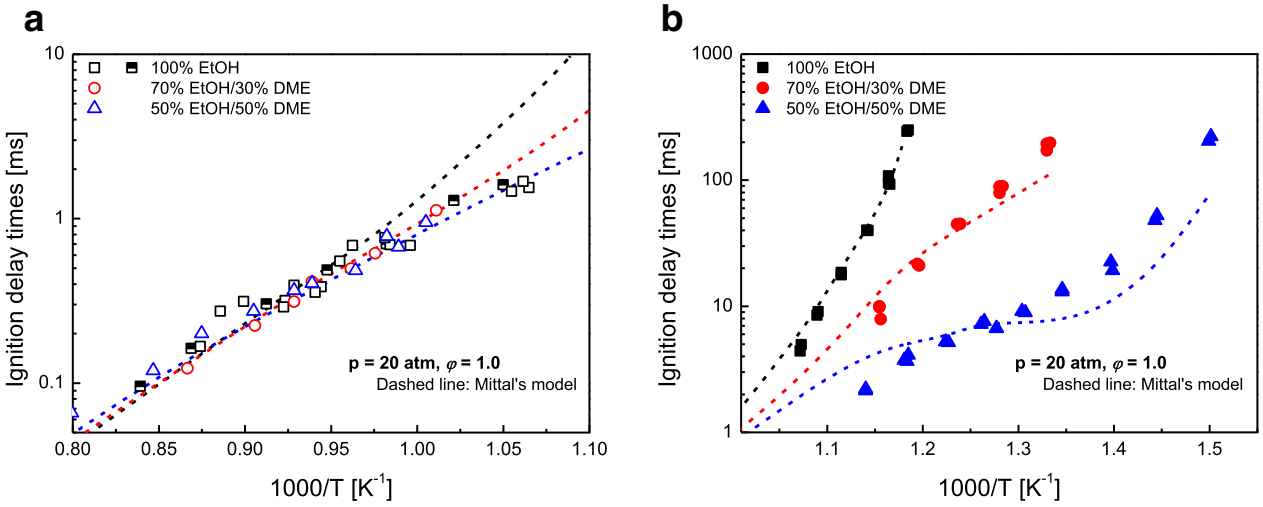

Fig. 2. Comparisons of experimental results and model predictions. Symbols represent the ignition delay times measured in this study, (a) shock tube, (b) rapid compression machine, and lines denote the simulations with Mittal's model [22].

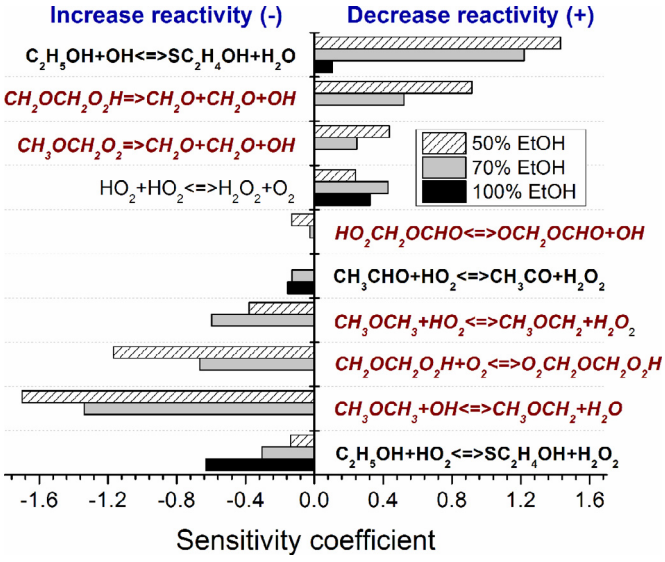

Fig. 3. "Brute-force" sensitivity analysis on ignition delay times performed at $p = 20$ atm, $\varphi = 1.0$ and $T = 770$ K for 100% EtOH, 70/30 and 50/50 EtOH/DME mixtures.

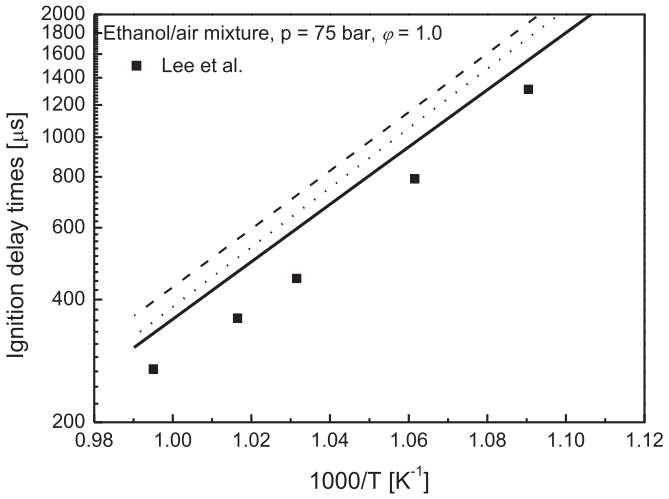

Fig. 4. Recent measurements of ignition delay times of ethanol at 75 bar [21]. Solid line: proposed model, dashed line: proposed model with Mittal's recommendation for reaction $C_2H_5OH + HO_2 = sC_2H_4OH + H_2O_2$, and dot line: Mittal et al.'s model [22].

shock waves. They found that the Sivaramakrishnan et al. calculation was in good agreement with the experiments for the total rate whereas the branching ratio of the beta site lay outside of their uncertainty bounds (BR_β was between 20 and 25% with 45% uncertainty at the temperature ranging from 900 to 1250 K). In contrast, Stranic et al.'s measurement does better agree with the Mittal et al. [22] recommendation. We therefore take the rate constant unchanged from Mittal et al. in our proposed model.

3.2. Fuel radical decomposition

Fuel radical (α-hydroxyethyl ($CH_3\dot{C}HOH$) and ethoxy ($C_2H_5\dot{O}$)) decomposition reactions are less important to simulate the high-pressure reactivity of ethanol measured in this study but they are important to describe ethanol pyrolysis measured in a flow reactor [24]. Several ab initio calculations are available in the literature, Metcalfe et al. [37], Xu et al. [56], Cai et al. [57] and Dames [58]. However, there appears to be no consensus for high- and low-pressure limits and this leads to a significant deviation in predicting the ethanol pyrolysis data, Fig. 5. Clearly, using the rate constants calculated by Dames leads to significantly better agreement with the pyrolysis data from Li et al. [24] especially ethanol and acetaldehyde, when compared to the other literature values. The main cause is that the rate constants calculated by Dames are performed at a higher level of theory with a more accurate one-dimensional potential energy surface and are in good agreement with the experimental data in the falloff region measured by Caralp et al. [59]. We have therefore selected Dames' calculations to describe the kinetics of the fuel radical decomposition reactions.

3.3. Reactions of O_2 addition to $\dot{C}H_2CH_2OH$ radical

In all of the literature kinetic mechanisms describing the oxidation of ethanol, the majority of β-hydroxyethyl radicals ($\dot{C}H_2CH_2OH$) undergo beta-scission forming ethylene, and only a small proportion (<9.0%) react with molecular O_2 to form peroxy-hydroxyethyl radicals ($CH_2CH_2OH–2\dot{O}_2$) followed by the Waddington type reaction pathway to form $\dot{O}H$ radicals and formaldehyde. Note that we have adopted the

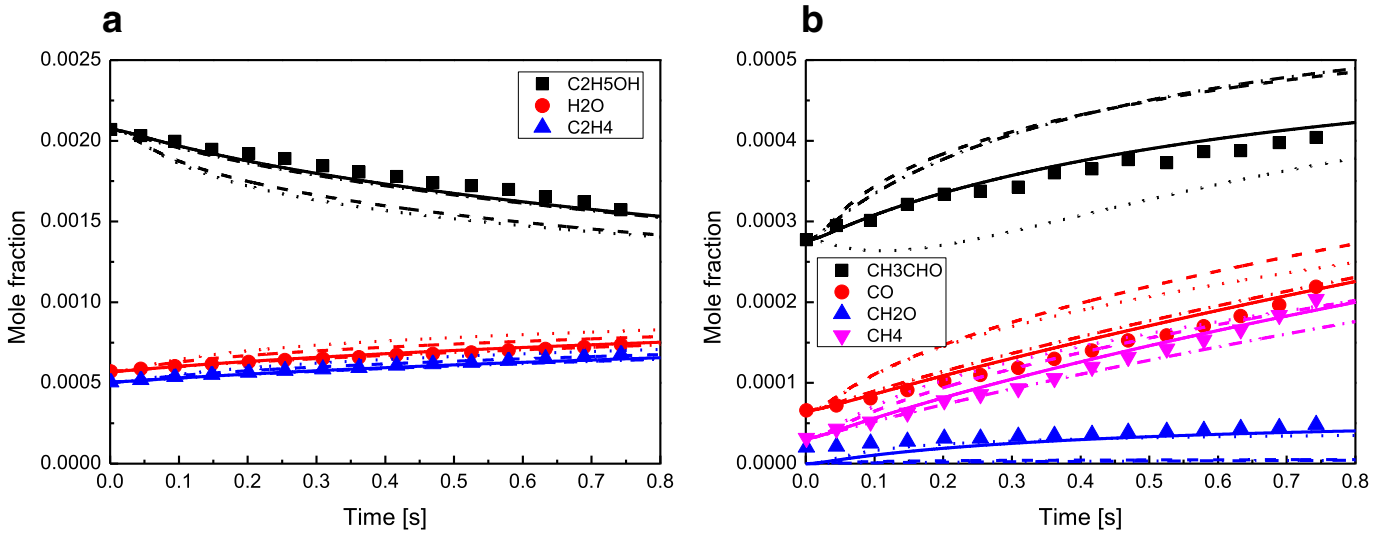

Fig. 5. Effect of fuel radical decomposition reactions from different sources on prediction in the species profiles (0.3 $C_2H_5OH + 0.0035\ O_2$ 99.6965 N_2 at 6.0 atm and 958 K, 1.5 s) [24]. Symbols represent experimental measurements; lines denote model simulations with Dames's calculations [58] (solid line), Metcalfe et al. [37] calculations (dash line), Xu et al. [56] calculations (dot line) and Cai et al. [57] calculations (dash dot line).

altered rate constants recommended by Mittal et al. [22] to describe the kinetic process of reactions $C_2H_5OH + \dot{O}H$ and generating reasonable quantities of $\dot{C}H_2CH_2OH$ radicals. However, there remains an over-prediction in simulating ethylene concentrations compared to the data measured at low temperatures by Leplat et al. [27]. A sensitivity analysis to intermediate species shows that ethylene formation is very sensitive to the Waddington mechanism ($CH_2CH_2OH\text{–}2\dot{O}_2 = CH_2O + CH_2O + \dot{O}H$). Recently, Sun et al. [60] implemented a thermochemical and kinetic analysis on the reactions of O_2 with products from $\dot{O}H$ addition to three radicals including isobutene, 2–hydroxy–1,1-dimethylethyl, and 2–hydroxy–2-methylpropyl at the CBS-Q//B3LYP level of theory. It was shown that the fuel radical ($C_2\dot{C}OH$) react with O_2 to form a chemically activated peroxyl adduct ($C_2C(O\dot{O})COH$) with a well depth of 38.9 kcal mol^{-1} to the lowest energy adduct intermediate. The adduct intermediate can dissociate to smaller and more stable products via a six-membered transition state ring, i.e. the Waddington mechanism. Here, we use the calculations performed on the $C_2\dot{C}OH + O_2$ system by Sun et al. and apply them to the $\dot{C}H_2CH_2OH + O_2$ system pertinent here for both the stabilization reaction and Waddington pathway. Figure 6 shows a comparison of the rate constants describing the $\dot{C}H_2CH_2OH + O_2$ kinetic process and illustrates the effect of the Waddington pathway on the ethylene formation profiles measured by Leplat et al. [27]. It can be seen that Mittal et al. [22] estimated a rate constant that is four times lower at 740 K than that calculated by Sun et al. for well stabilization, and the Mittal et al. estimate for the Waddington reaction is four orders of magnitude lower at 670 K compared to that from Sun et al. [60], Fig. 6(a). Thus, in the Mittal et al. mechanism $\dot{C}H_2CH_2OH$ radical addition to molecular oxygen is unable to compete with $\dot{C}H_2CH_2OH$ radical beta-scission at low temperatures. Moreover, increasing the rate constant of the Waddington reaction within a factor of two significantly reduces the formation of ethylene but this effect appears to be more dramatic at lower temperatures ($T < 950$ K), Fig. 6(b). Clearly, the proposed model using the Sun et al. calculations is in better agreement with the Leplat et al. [27] experiments relative to the model presented by Mittal et al. [22].

In addition, Sun et al. [60] pointed out an alternative isomerization reaction path for the $C_2C(O\dot{O})COH$ adduct via H-atom transfer from the alcohol carbon via a five-membered transition state ring to form the $C_2C(OOH)\dot{C}OH$ radical with an energy barrier of 28.4 kcal mol^{-1}. Subsequently, the $C_2C(OOH)\dot{C}OH$ radical undergoes either intramolecular substitution via a three-membered transition state ring to form the three-membered ring epoxides $(cy(CCO)COH) + \dot{O}H$ or undergo an $H\dot{O}_2$ concerted elimination to form olefinic alcohols, $C_2C{=}COH$. However, these kinetic processes have not been included in all of the previous literature ethanol mechanisms. To further explore their effect, an analogous analysis to the Sun et al. [60] study has been made to describe the kinetic process of $CH_2CH_2OH\text{–}2\dot{O}_2$ decomposition via $H\dot{O}_2$ elimination and ring epoxides formation. Figure 7 shows the effect on ethylene formation of these new additional reactions. It is clear that the addition of the new reactions inhibits ethylene formation at lower temperatures (950 K), resulting in a better agreement with the experimental measurements [27]. Note that the modification of the Waddington mechanism and the addition of these new reactions does not impact the overall reactivity of ethanol and/or ethanol/DME mixtures reported here, but they do influence ethylene predictions.

3.4. Carbonyl-hydroperoxide decomposition

Adjusting the rate constants of the reactions discussed above did not resolve the problem of the model's under-prediction of measured ignition delay times for the 50%/50% EtOH/DME mixtures. It is obvious that with increasing concentrations of DME, the reactions controlling ignition kinetic gradually transition to DME chemistry. The rate constants related to DME low temperature chemistry highlighted in Fig. 3 has been carefully optimized by Burke et al. [48]. However, the decomposition of carbonyl-hydroperoxide (HO_2CH_2OCHO) forming $\dot{O}CH_2OCHO$ and $\dot{O}H$ radicals still has a large uncertainty. The rate constant was originally adopted from Sahetchian et al. [61] ($k = 1 \times 10^{16} \exp(-43000/RT)$) and used by Burke et al. [48], Curran et al. [62,63] and Zhao et al. [64], with these authors increasing the rate constant recommended by Sahetchian et al. by factors of 5, 10 and 24, respectively. To achieve better model predictions of the reactivity of EtOH/DME mixtures, we increase the rate constant of Sahetchian et al. by a factor of 2.5, which is within the uncertainty of their measurement. Figure 8 shows comparisons of the model performance before and after changing the rate constant

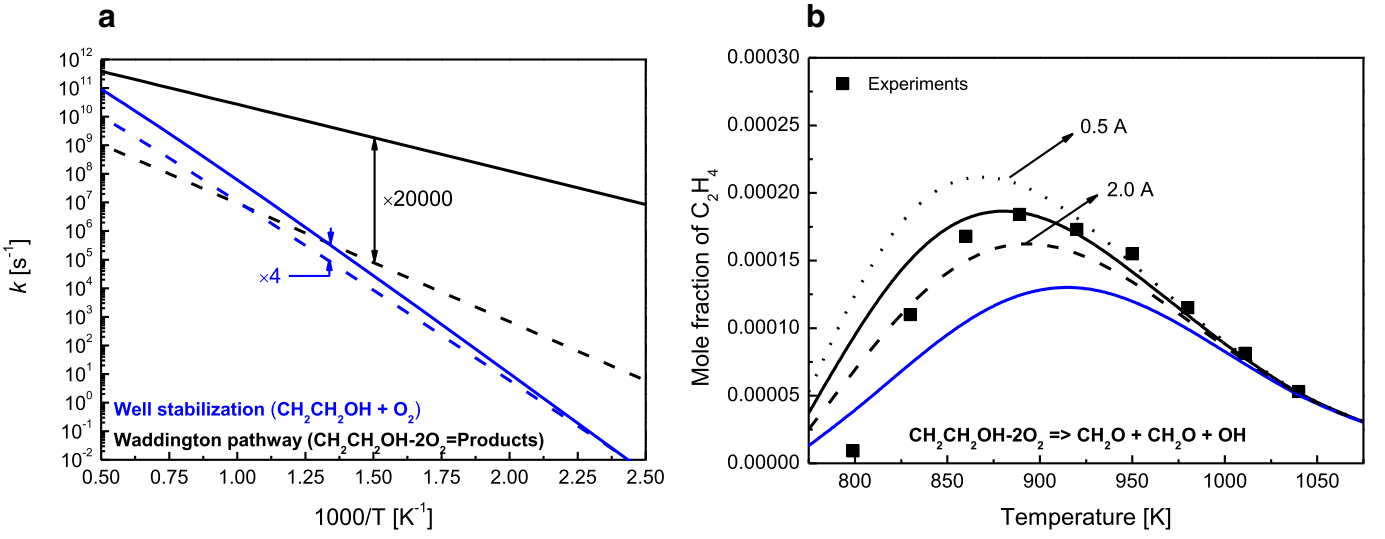

Fig. 6. Effect of Waddington reaction pathway on the C_2H_4 concentration at low temperatures. (a) Comparison of rate constants of the $\dot{C}H_2CH_2OH + O_2$ kinetic process. Solid line: rate constants from Sun et al. [60] and dash line: rate constants from Mittal et al. [22]. (b) Comparison of Waddington reaction pathway on JSR C_2H_4 formation (0.2 $C_2H_5OH + 2.0\ O_2 + 97.8\ N_2$ at 10 atm, $\varphi = 0.3$). Symbols represent experimental measurements from Leplat et al. [27]. Lines denote model simulations. Black solid line: new Waddington mechanism from this study, black dash line: 2 × A-factor of the Waddington pathway, black dot line: 0.5 × A-factor of the Waddington pathway and blue solid line: old Waddington mechanism from Mittal et al. (For interpretation of the references to colour in this figure legend, the reader is referred to the web version of this article).

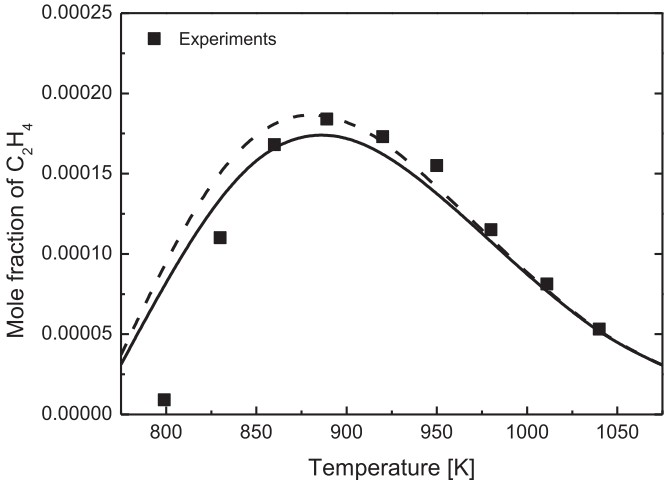

Fig. 7. Effects of $H\dot{O}_2$ concerted elimination and ring epoxides formation on the C_2H_4 concentration at low temperatures. Symbols represent experimental measurements from Leplat et al. [27] (0.2 $C_2H_5OH + 2.0\ O_2 + 97.8\ N_2$ at 10 atm, $\varphi = 0.3$). Lines denote model simulations. Solid line: proposed model with new Waddington mechanism + additional reactions from this study and dash line: proposed model with new Waddington mechanism only.

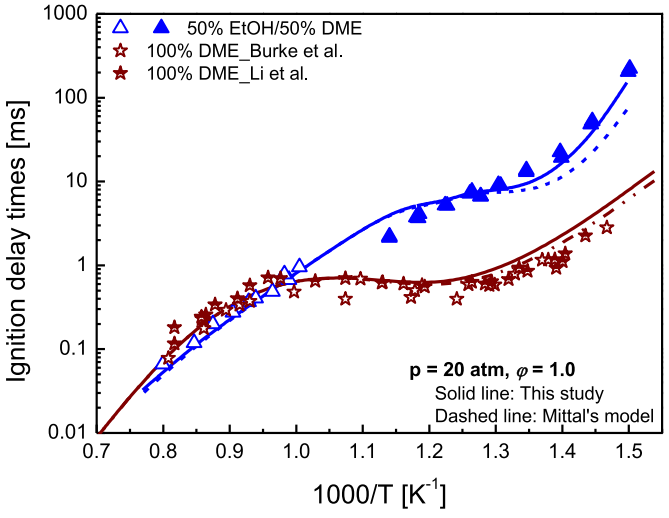

Fig. 8. Effect of reaction $HO_2CH_2OCHO = \dot{O}CH_2OCHO + \dot{O}H$ on the low-temperature reactivity of 50/50 EtOH/DME mixture at $p = 20$ atm and $\varphi = 1.0$ (Burke et al. [48], Li et al. [65], Mittal et al. [22]).

of $HO_2CH_2OCHO = \dot{O}CH_2OCHO + \dot{O}H$. For the 50%/50% EtOH/DME mixture, the change has no effect on the reactivity at temperatures over 800 K but it increases the ignition delay times by a factor of 1.7 and 2.3 at 700 K and 667 K, respectively. Note that this change did not influence the reactivity of pure EtOH and the 70% EtOH/30% DME mixtures but results in a much better prediction of the ignition delay times measured for the 50% EtOH/50% DME and pure DME mixtures.

3.5. Updated model performance

The proposed chemical kinetic mechanism has been validated by comparing against experimental data taken in multiple devices including ignition delay times [19–23,28,29], JSR [27] and flow reactor [24,26,66,67] species profiles, over a wide range of pressure, temperature, and fuel/oxidizer conditions. Only typical cases (Figs. 9–11) have been selected here to verify the model performance and more detail validations are available as Supplementary Material. In general, the proposed model is in good agreement with all of the experimental targets. There are two highlights in the model validations: (a) literature mechanisms for ethanol [22,35,37,66] are capable of capturing the ignition delay times at pressures below 40 atm for fuel in air mixtures whereas all of them significantly over-predict the reactivity at high pressures (75 atm) measured by Lee et al. [21] which we believe may be due to the use of a slightly low rate constant for the reaction: $C_2H_5OH + H\dot{O}_2 = CH_3\dot{C}HOH + H_2O_2$ used in those models. In contrast, the model presented here shows very good agreement with the experimental data—for both fuel in air mixtures and fuel in argon mixtures not only at lower pressures but also at high pressures, (Fig. 9a), despite the fact that the Mittal et al. [22] model can quite accurately simulate fundamental combustion targets, the predictions in the evolution of ethylene measured in both a JSR

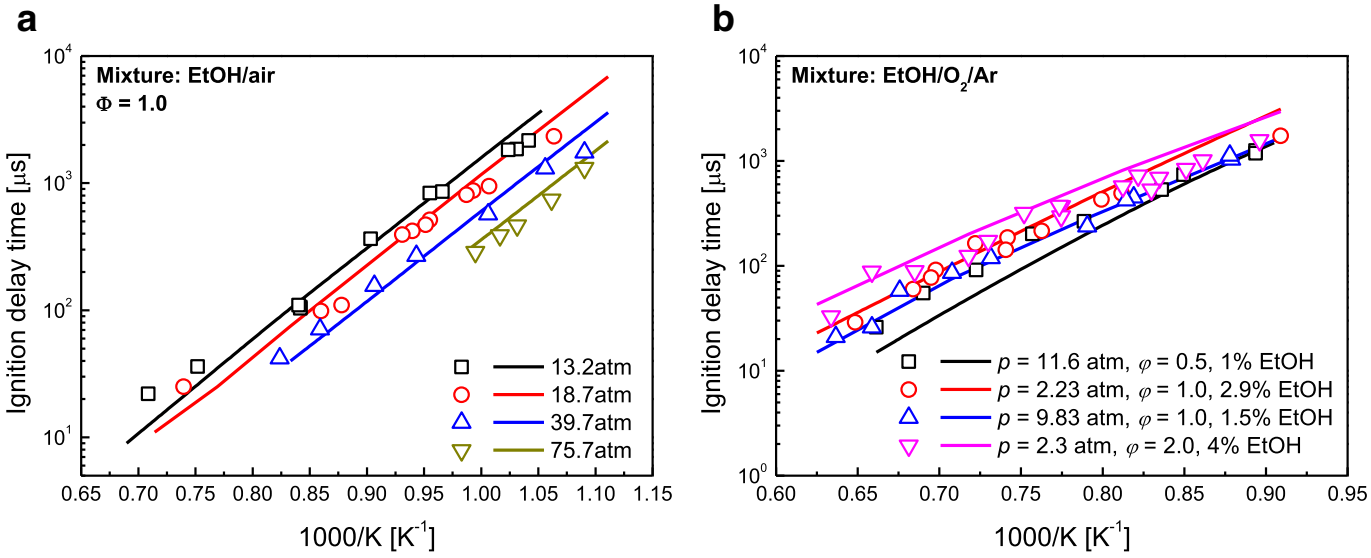

Fig. 9. Ignition delay time validation. Symbols represent experiments and lines denote proposed model predictions. (a) Model performance in predicting high pressure data for fuel in air mixtures taken from Heufer and Olivier [19] and Lee et al. [21]. (b) Model performance in predicting lower pressure data for fuel in argon mixtures taken from Noorani et al. [28].

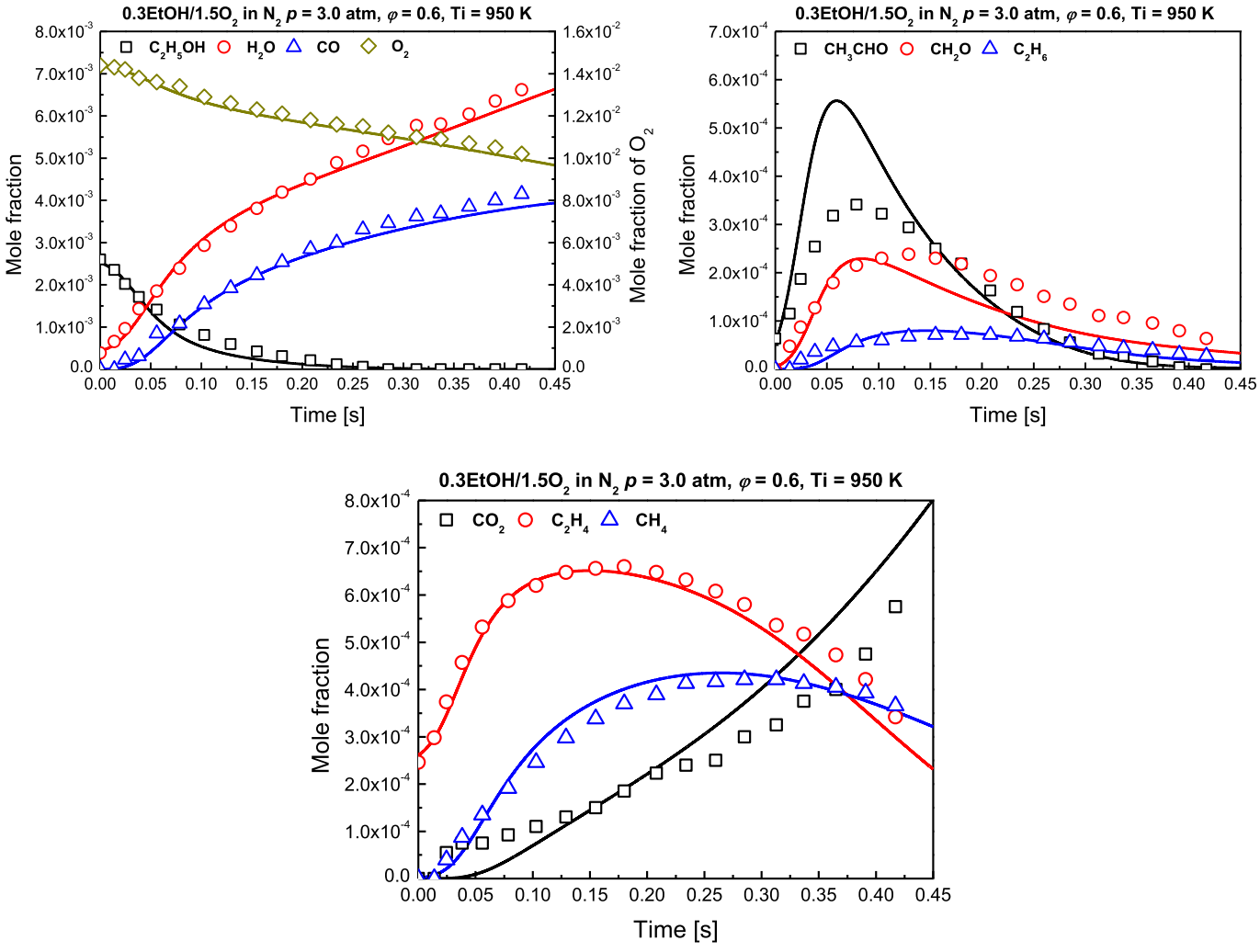

Fig. 10. Flow reactor speciation validation. Symbols: experiments [66]. Lines: proposed model predictions.

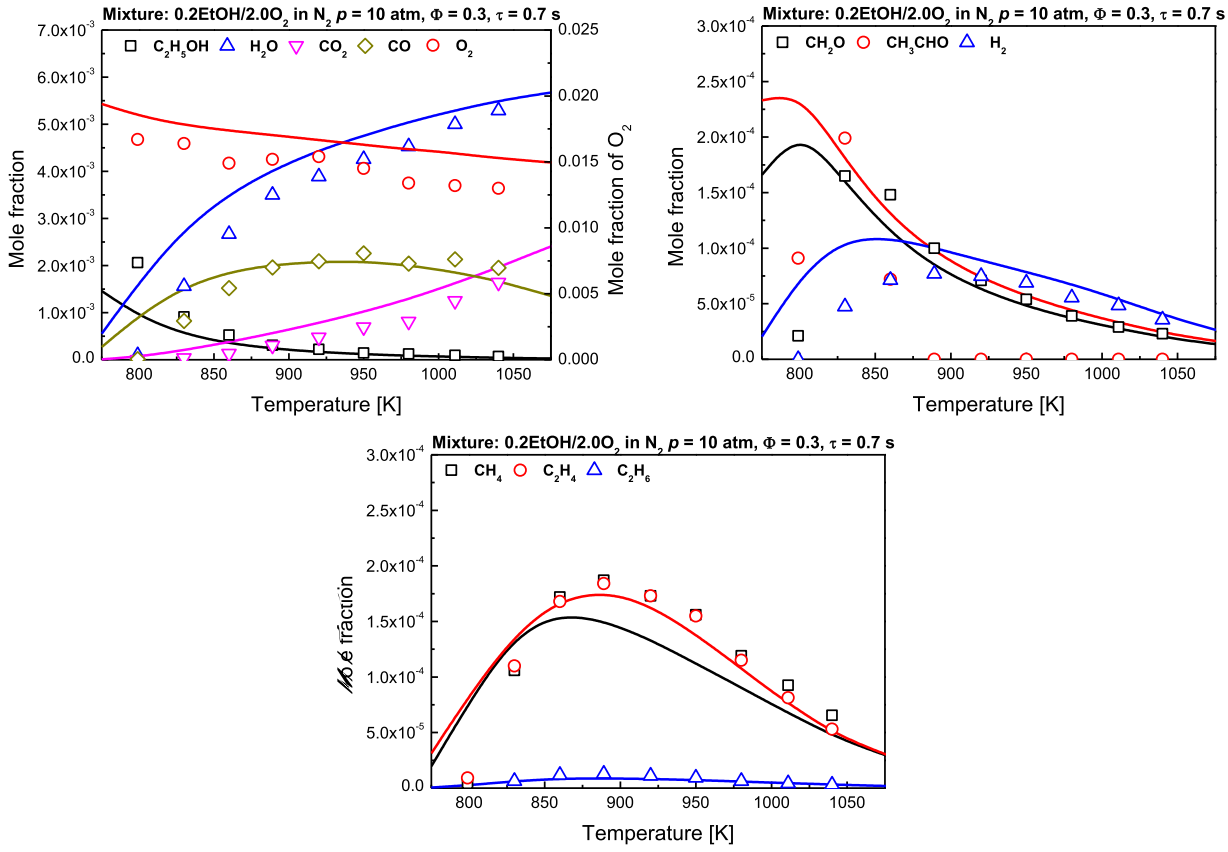

Fig. 11. Jet-stirred reactor speciation validation. Symbols: experiments [27]. Lines: proposed model predictions.

[27] and in a flow reactor [66] are inaccurate due to (i) the incomplete description of relatively important reactions (fuel radical decomposition and O_2 addition to $\dot{C}H_2CH_2OH$) and (ii) the rate constant of the Waddington pathway improperly estimated in the Mittal et al. [22] model. Cleary, ethylene profiles are well predicted by the proposed model via the refinements made in the low-temperature kinetics of ethanol.

4. Results and discussion

All mixtures were tested in the RCM in order to measure the ignition delay times in the low temperature range. For the experiments at higher temperatures, they were performed in the DRIVE-HPST except for the DME mixtures which were previously measured in the NUIG HPST [48]. Moreover, the 100% EtOH mixtures at 20 and 40 atm and at $\varphi = 1.0$ were studied in both facilities to allow an inter-comparison of experimental results, with good agreement observed. All of the experimental data are available as Supplementary Material.

4.1. Effect of physical conditions on reactivity of pure fuels

Generally, for the mixtures with a given blending ratio, the experimental trends with respect to the influence on ignition delay time of temperature, pressure and equivalence ratio are very much in-line with chemical intuition and will not be discussed in great detail here. The extreme cases of 100% EtOH and 100% DME ignition will be briefly described to highlight the antagonistic behavior of EtOH on DME and/or the promoting effect of DME on EtOH and to provide a basis for discussion of the behavior of the fuel blends. All of the measured and simulated ignition delay times are provided in Fig. 13.

For the pure EtOH mixtures the experimental temperature dependence can be essentially correlated using an Arrhenius or

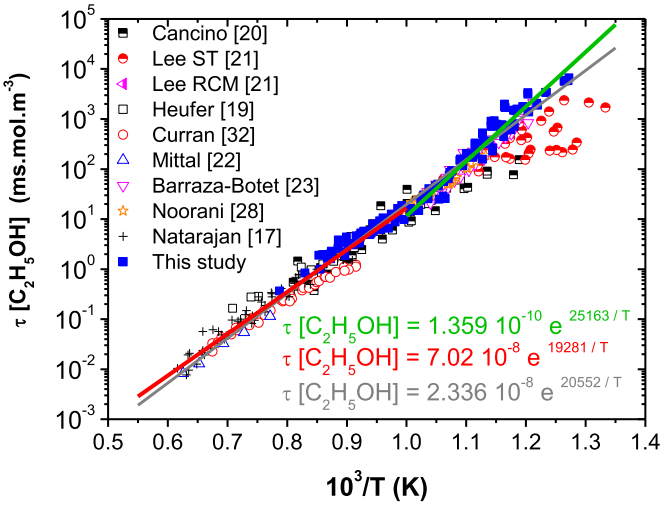

Fig. 12. Comparison of the literature [17,19–23,28,32] and current ignition delay time data multiplied by the molar concentration of ethanol (symbols: experimental data, lines: correlations calculated over the full temperature range —, the low temperature range – and the high temperature range —).

modified-Arrhenius type correlation in both the high- and low-temperature regimes without a change in the global activation energy. This is true for all conditions of pressure and equivalence ratio. As recently presented by Mittal et al. [22] and Barraza-Botet et al. [23], the experimental results obtained in the present study have been plotted against previous experimental data from the literature (Fig. 1(a)), Fig. 12. However, in the present study, the ignition delay times have been multiplied by the molar concentration of ethanol in order to remove the impacts of dilution and equiv-

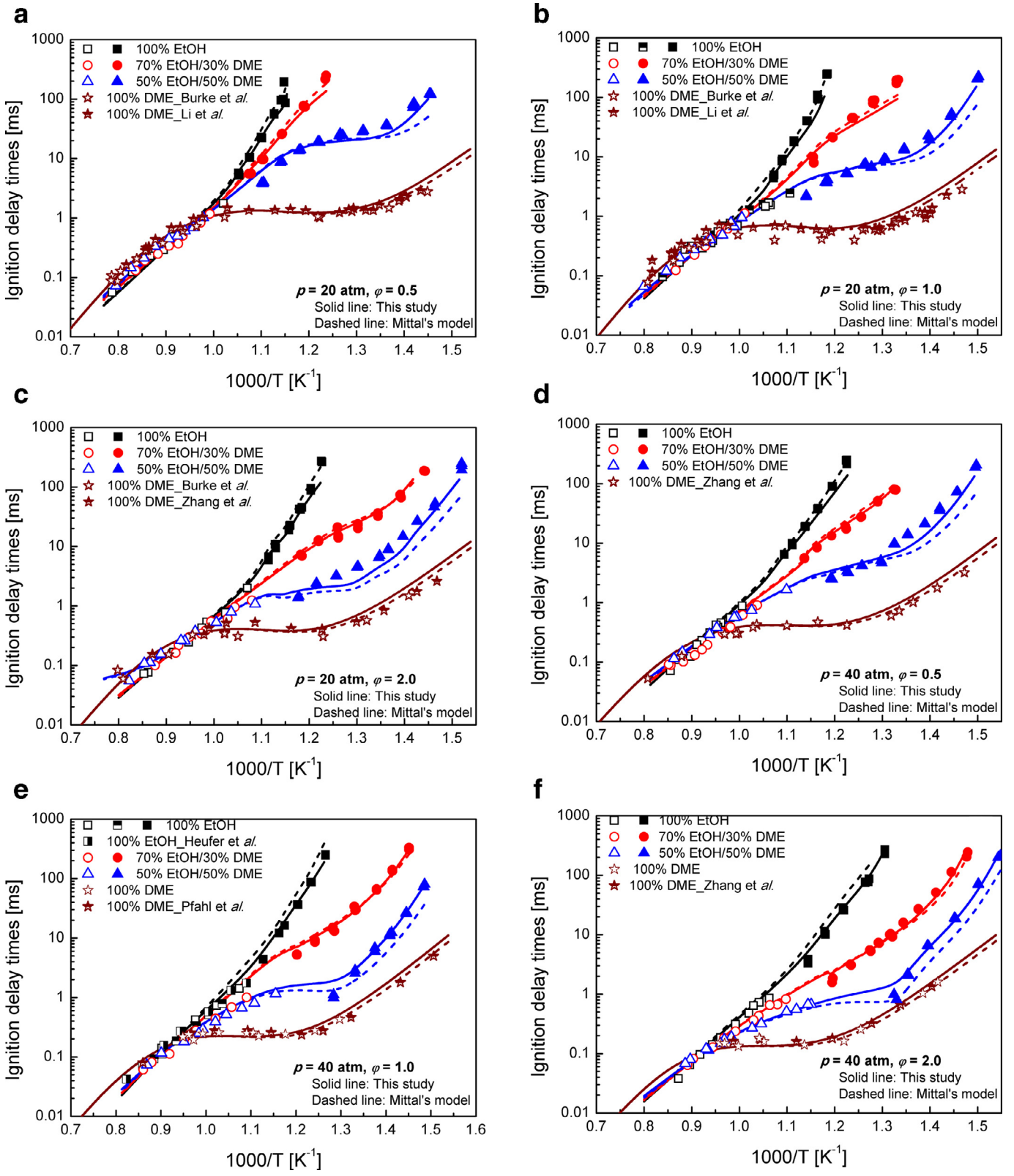

Fig. 13. Effect of varying blending ratio on the reactivity of EtOH/DME mixtures with the simulation comparison of proposed and Mittal's model [22] and comparison with previously published experimental data [19,38,48,65].

alence ratio. A perfect agreement is obtained between all of the datasets, expect for the low temperature data from Lee et al. [21]. These data are shorter than expected due to in-homogeneous ignition and pre-ignition pressure rise as explained by Lee et al. in their paper. A correlation has been calculated for all the datasets excluding the Lee et al. data. The line and the equation presented in Fig. 12 represent this correlation. However, such a correlation does not reflect the opposing facility effects encountered in the shock tube and in the RCM. These facility effects, pre-ignition pressure rise in the shock tube and heat losses in the RCM, result

in shorter measured ignition delay times in the shock tube and longer ignition delay times in the RCM compared to those expected under more ideal conditions. Therefore, the data have been split into two groups, namely those below and above 1000 K and two new correlations have been calculated. It can be seen that better agreement is obtained with the data in the low- and intermediate-temperature range and this results in a higher activation energy. However, this creates a discontinuity at 1000 K.

Both the updated and original mechanisms can predict the Arrhenius-type behavior with very little difference between them, as under the conditions studied, EtOH shows little or no reactivity at temperatures below 900 K. Hence our need to use a highly-reactive radical initiator, DME, to induce low temperature chemistry in order to shorten ignition times and permit the measurement of ignition delay times.

For 100% DME the ignition delay times show a straightforward Arrhenius-type dependence at temperatures above approximately 1050 K, whereas at temperatures below this a typical NTC behavior can be observed due to DME's well-established chain-branching reaction mechanism. Again, both models accurately simulate this behavior.

It is clear that the original and updated models can predict ignition times for ethanol/air mixtures at temperatures above 850 K and DME/air mixtures over the entire temperature ranges investigated, for all conditions of pressures and equivalence ratios. The fundamental question of this work now arises. Do the models retain their predictability for the experimental measurements beyond the previous validation ranges studied?

4.2. Effect of blending ratio on reactivity

Our results indicate that, the addition of DME exhibits a two-fold effect on ethanol ignition: (1) DME inhibits the reactivity of ethanol at higher temperatures ($T > 1050$ K) as ethanol undergoes either unimolecular decomposition or beta-H atom abstraction to form the highly reactive species, ethylene and $\dot{O}H$ radicals, which results in accelerated ignition. By contrast at high temperatures, only relatively unreactive species, namely $\dot{C}H_3$ radicals and formaldehyde are formed in DME oxidation via either unimolecular decomposition or H-atom abstraction followed by C–O beta scission, resulting in the inhibition of ignition; (2) DME promotes the reactivity of ethanol at lower temperatures ($T = 650$–950 K) where ethanol mainly undergoes alpha-H atom abstraction followed by O–H bond β-scission forming less-reactive acetaldehyde while DME can undergo the low temperature chain-branching process to form abundant $\dot{O}H$ radicals. As a result, DME addition enhances reactivity at lower temperatures, as shown in Fig. 13. We have also considered four types of cross reactions, including:

$$C_2H_5OH + \dot{R} = \dot{C}H_2CH_2OH/CH_3\dot{C}HOH + RH$$

$$C_2H_5OH + R\dot{O}_2 = \dot{C}H_2CH_2OH/CH_3\dot{C}HOH + ROOH$$

$$C_2H_5OH + \dot{O}OOH = \dot{C}H_2CH_2OH/CH_3\dot{C}HOH + ROOH$$

$$C_2H_5OH + \dot{O}_2QOOH = \dot{C}H_2CH_2OH/CH_3\dot{C}HOH + 2CH_2O + H\dot{O}_2 + \dot{O}H$$

where, $\dot{R}$ is the DME radical ($CH_3O\dot{C}H_2$). The corresponding rate constants were taken from analogies with $C_2H_5OH + \dot{C}_2H_5$ for assigning R1 and R3 and $C_2H_5OH + CH_3\dot{O}_2$ for assigning R2 and R4, respectively.

Similar to our previous work on toluene/DME mixtures [38], these cross reactions have no effect on the reactivity of all EtOH/DME mixtures and on species profiles measured during EtOH oxidation. However, we are unsure whether the cross reactions have an effect on the speciation profiles measured during DME oxidation, particularly those with high mole fractions of DME.

Interestingly, the 70%/30% EtOH/DME mixtures retain the ignition behavior of ethanol suggesting that ethanol chemistry dominants the ignition kinetics of these mixture even though more reactions involving DME chemistry appear in the sensitivity analysis, Fig. 3. Both models reproduce well the experimental observations. For the 50%/50% EtOH/DME mixtures, the ignition behavior is closer to that of pure DME, showing NTC behavior. The original model is capable of predicting the experimental data at temperatures above 910 K but it under-predicts the reactivity at temperature below 910 K. Obviously, the modification in the reaction of HO_2CH_2OCHO decomposition improves agreement in terms of the measured reactivity of the binary fuel mixtures.

5. Conclusions

Ignition delay times for ethanol/DME/air blends have been measured in shock tube and RCM facilities under a wide-range of conditions relevant to internal combustion engines. Generally, for a given pure-mixture, the experimental trends with respect to the impact of temperature, pressure and equivalence ratio are in-line with past-studies. However, the addition of DME to EtOH exhibits a distinctly different effect on its reactivity in the high- and low-temperature regimes. At temperatures above 1100 K, no significant change in the ignition delay times of ethanol can be found. At temperatures below 1100 K, DME significantly promotes the reactivity of ethanol, particularly in the NTC regime due to the accumulation of abundant $\dot{O}H$ radicals via the low-temperature chain branching mechanism of DME. When the proportion of DME is less 30%, no obvious NTC behavior can be found in the ignition process of ethanol/DME mixtures at all conditions, meaning that the measured temperature range can be extended to 685 K for the 70%/30% ethanol/DME mixture at 40 atm at fuel-rich conditions while still retaining the ethanol controlling kinetics. However, when the proportion of DME is above 30%, the experimental observation shows a DME-like ignition behavior, suggesting that ignition is dominated by DME chemistry.

A literature binary-fuel mechanism is not capable of predicting the ignition behavior of the ethanol/DME mixtures over the complete range of temperatures, pressures and equivalence ratios and blending ratios studied here especially for the 50%/50% mixtures at lower temperatures (<800 K). The novel observation has allowed us to gain a critical insight into the low-temperature chemistry of the binary mixtures. Asides from the new experimental database, a key outcome of the current work is an updated chemical kinetic model. Specifically, the rate constant for H-atom abstraction from the beta site on ethanol by $H\dot{O}_2$ radical is refined to better-predict the high-pressure reactivity of ethanol. The kinetic process of fuel radical decomposition is re-established via incorporating the latest theoretical calculations to better describe the pyrolysis of ethanol and low-pressure ignition delay times. More reasonable rate constants are assigned to describe the kinetics of $P\dot{O}_2H_4OH + O_2$ reactions, and the orders of magnitude differences in the rate constants of the Waddington pathways and O_2 addition are responsible for the inability of the original mechanism to predict the evolution of ethylene at lower temperatures. Our new proposed mechanism is better able to capture the new experimental data and literature measurements.

Acknowledgments

The work at Xi'an Jiaotong University was supported by the National Natural Science Foundation of China (no. 91541115) and the Fundamental Research Funds for the Central Universities. The work at DRIVE laboratory was supported by French National Research Agency under the ANR project SHOCK (ANR-13-JS09-0013-01) and the Council of Burgundy (Project STM3D).

Supplementary materials

Supplementary material associated with this article can be found, in the online version, at doi:10.1016/j.combustflame.2017.11.011.

References

[1] P.S. Nigam, A. Singh, Production of liquid biofuels from renewable resources, Prog. Energy Combust. Sci. 37 (2011) 52–68, doi:10.1016/j.pecs.2010.01.003.
[2] A. Demirbas, Progress and recent trends in biofuels, Prog. Energy Combust. Sci. 33 (2007) 1–18, doi:10.1016/j.pecs.2006.06.001.
[3] M. Wu, Y. Wu, M. Wang, Energy and emission benefits of alternative transportation liquid fuels derived from switchgrass: a fuel life cycle assessment, Biotechnol. Progr. 22 (2006) 1012–1024, doi:10.1021/bp050371p.
[4] B.L. Salvi, K.A. Subramanian, N.L. Panwar, Alternative fuels for transportation vehicles: a technical review, Renewable Sustainable Energy Rev. 25 (2013) 404–419, doi:10.1016/J.RSER.2013.04.017.
[5] L. Tock, M. Gassner, F. Maréchal, Thermochemical production of liquid fuels from biomass: thermo-economic modeling, process design and process integration analysis, Biomass Bioenergy 34 (2010) 1838–1854, doi:10.1016/J.BIOMBIOE.2010.07.018.
[6] V. Gargiulo, M. Alfè, G. Di Blasio, C. Beatrice, Chemico-physical features of soot emitted from a dual-fuel ethanol–diesel system, Fuel 150 (2015) 154–161, doi:10.1016/j.fuel.2015.01.096.
[7] M. Matti Maricq, Soot formation in ethanol/gasoline fuel blend diffusion flames, Combust. Flame 159 (2012) 170–180, doi:10.1016/j.combustflame.2011.07.010.
[8] C. Arcoumanis, C. Bae, R. Crookes, E. Kinoshita, The potential of di-methyl ether (DME) as an alternative fuel for compression-ignition engines: a review, Fuel 87 (2008) 1014–1030, doi:10.1016/J.FUEL.2007.06.007.
[9] F.M. Haas, M. Chaos, F.L. Dryer, Low and intermediate temperature oxidation of ethanol and ethanol–PRF blends: an experimental and modeling study, Combust. Flame 156 (2009) 2346–2350, doi:10.1016/j.combustflame.2009.08.012.
[10] Ö.L Gülder, Laminar burning velocities of methanol, ethanol and isooctane-air mixtures, Symp. (Int.) Combust. 19 (1982) 275–281, doi:10.1016/S0082-0784(82)80198-7.
[11] F.N. Egolfopoulos, D.X. Du, C.K. Law, A study on ethanol oxidation kinetics in laminar premixed flames, flow reactors, and shock tubes, Symp. (Int.) Combust. 24 (1992) 833–841, doi:10.1016/S0082-0784(06)80101-3.
[12] T.S. Kasper, P. Oßwald, M. Kamphus, K. Kohse-Höinghaus, Ethanol flame structure investigated by molecular beam mass spectrometry, Combust. Flame 150 (2007) 220–231, doi:10.1016/j.combustflame.2006.12.022.
[13] K. Eisazadeh-Far, A. Moghaddas, J. Al-Mulki, H. Metghalchi, Laminar burning speeds of ethanol/air/diluent mixtures, Proc. Combust. Inst. 33 (2011) 1021–1027, doi:10.1016/j.proci.2010.05.105.
[14] G. Broustail, P. Seers, F. Halter, G. Moréac, C. Mounaim-Rousselle, Experimental determination of laminar burning velocity for butanol and ethanol iso-octane blends, Fuel 90 (2011) 1–6, doi:10.1016/j.fuel.2010.09.021.
[15] P. Saxena, F.A. Williams, Numerical and experimental studies of ethanol flames, Proc. Combust. Inst. 31 (2007) 1149–1156, doi:10.1016/j.proci.2006.08.097.
[16] E. Varea, V. Modica, A. Vandel, B. Renou, Measurement of laminar burning velocity and Markstein length relative to fresh gases using a new postprocessing procedure: application to laminar spherical flames for methane, ethanol and isooctane/air mixtures, Combust. Flame 159 (2012) 577–590, doi:10.1016/j.combustflame.2011.09.002.
[17] K. Natarajan, K.A. Bhaskaran, An experimental and analytical investigation of high temperature ignition of ethanol, Proc. 13th Internatinal Symp. Shock Tubes Waves (1981), pp. 834–842.
[18] M.P. Dunphy, J.M. Simmie, High-temperature oxidation of ethanol. Part 1—ignition delays in shock waves, J. Chem. Soc. Faraday Trans. 87 (1991) 1691–1696.
[19] K.A. Heufer, H. Olivier, Determination of ignition delay times of different hydrocarbons in a new high pressure shock tube, Shock Waves 20 (2010) 307–316, doi:10.1007/s00193-010-0262-2.
[20] L.R. Cancino, M. Fikri, A.A.M. Oliveira, C. Schulz, Measurement and chemical kinetics modeling of shock-induced ignition of ethanol–air mixtures, Energy Fuels 24 (2010) 2830–2840, doi:10.1021/ef100076w.
[21] C. Lee, S. Vranckx, K.A. Heufer, S.V. Khomik, Y. Uygun, H. Olivier, R.X. Fernandez, On the chemical kinetics of ethanol oxidation: shock tube, rapid compression machine and detailed modeling study, Z. Phys. Chem. 226 (2012) 1–28, doi:10.1524/zpch.2012.0185.
[22] G. Mittal, S.M. Burke, V.A. Davies, B. Parajuli, W.K. Metcalfe, H.J. Curran, Autoignition of ethanol in a rapid compression machine, Combust. Flame 161 (2014) 1164–1171, doi:10.1016/j.combustflame.2013.11.005.
[23] C.L. Barraza-Botet, S.W. Wagnon, M.S. Wooldridge, Combustion chemistry of ethanol: ignition and speciation studies in a rapid compression facility, J. Phys. Chem. A 120 (2016) 7408–7418, doi:10.1021/acs.jpca.6b06725.
[24] J. Li, A. Kazakov, F.L. Dryer, Ethanol pyrolysis experiments in a variable pressure flow reactor, Int. J. Chem. Kinet. 33 (2001) 859–867, doi:10.1002/kin.10009.
[25] J. Li, A. Kazakov, F.L. Dryer, Experimental and numerical studies of ethanol decomposition reactions, J. Phys. Chem. A 108 (38) (2004) 7671–7680, doi:10.1021/JP0480302.
[26] F. Herrmann, B. Jochim, P. Oßwald, L. Cai, H. Pitsch, K. Kohse-Höinghaus, Experimental and numerical low-temperature oxidation study of ethanol and dimethyl ether, Combust. Flame 161 (2014) 384–397, doi:10.1016/j.combustflame.2013.09.014.
[27] N. Leplat, P. Dagaut, C. Togbé, J. Vandooren, Numerical and experimental study of ethanol combustion and oxidation in laminar premixed flames and in jet-stirred reactor, Combust. Flame 158 (2011) 705–725, doi:10.1016/j.combustflame.2010.12.008.
[28] K.E. Noorani, B. Akih-Kumgeh, J.M. Bergthorson, Comparative high temperature shock tube ignition of C1−C4 primary alcohols, Energy Fuels 24 (2010) 5834–5843, doi:10.1021/ef1009692.
[29] F.R. Gillespie, An experimental and modelling study of the combustion of oxygenated hydrocarbons, NUI Galway, 2014.
[30] D.C. Rakopoulos, C.D. Rakopoulos, R.G. Papagiannakis, D.C. Kyritsis, Combustion heat release analysis of ethanol or n-butanol diesel fuel blends in heavy-duty DI diesel engine, Fuel 90 (2011) 1855–1867, doi:10.1016/j.fuel.2010.12.003.
[31] S. Padala, C. Woo, S. Kook, E.R. Hawkes, Ethanol utilisation in a diesel engine using dual-fuelling technology, Fuel 109 (2013) 597–607, doi:10.1016/j.fuel.2013.03.049.
[32] H.J. Curran, M.P. Dunphy, J.M. Simmie, C.K. Westbrook, W.J. Pitz, Shock tube ignition of ethanol, isobutene and MTBE: experiments and modeling, Symp. (Int.) Combust. 24 (1992) 766–769.
[33] C. Olm, T. Varga, É. Valkó, S. Hartl, C. Hasse, T. Turányi, Development of an ethanol combustion mechanism based on a hierarchical optimization approach, Int. J. Chem. Kinet. 48 (2016) 423–441, doi:10.1002/kin.20998.
[34] M.P. Dunphy, P.M. Patterson, J.M. Simmie, High-temperature oxidation of ethanol. Part 2—kinetic modelling, J. Chem. Soc. Faraday Trans. 87 (1991) 2549–2559, doi:10.1039/FT9918702549.
[35] N.M. Marinov, A detailed chemical kinetic model for high temperature ethanol oxidation, Int. J. Chem. Kinet. 31 (1999) 183–220, doi:10.1002/(SICI)1097-4601(1999)31:3⟨183::AID-KIN3⟩3.0.CO;2-X.
[36] G.P. Smith, D.M. Golden, M. Frenklach, N.W. Moriarty, B. Eiteneer, M. Goldenberg, T. Bowman, R.K. Hanson, S. Song, J.W.C. Gardiner, V. Lissianski, Z. Qin, http://www.me.berkeley.edu/gri_mech/, (n.d.).
[37] W.K. Metcalfe, S.M. Burke, S.S. Ahmed, H.J. Curran, A hierarchical and comparative kinetic modeling study of C_1-C_2 hydrocarbon and oxygenated fuels, Int. J. Chem. Kinet. 45 (2013) 638–675, doi:10.1002/kin.20802.
[38] Y. Zhang, K.P. Somers, M. Mehl, W.J. Pitz, R.F. Cracknell, H.J. Curran, Probing the antagonistic effect of toluene as a component in surrogate fuel models at low temperatures and high pressures. A case study of toluene/dimethyl ether mixtures, Proc. Combust. Inst. 36 (2017) 413–421, doi:10.1016/j.proci.2016.06.190.
[39] L. Brett, J. MacNamara, P. Musch, J.M. Simmie, Simulation of methane autoignition in a rapid compression machine with creviced pistons, Combust. Flame 124 (2001) 326–329.
[40] S.M. Gallagher, H.J. Curran, W.K. Metcalfe, D. Healy, J.M. Simmie, G. Bourque, A rapid compression machine study of the oxidation of propane in the negative temperature coefficient regime, Combust. Flame 153 (2008) 316–333.
[41] J. Würmel, J.M. Simmie, CFD studies of a twin-piston rapid compression machine, Combust. Flame 141 (2005) 417–430.
[42] C. Morley, Gaseq version 0.79, 2005 Http://www.gaseq.co.uk/.
[43] D. Darcy, H. Nakamura, C.J. Tobin, M. Mehl, W.K. Metcalfe, W.J. Pitz, C.K. Westbrook, H.J. Curran, A high-pressure rapid compression machine study of n-propylbenzene ignition, Combust. Flame 161 (2014) 65–74.
[44] C. Lee, A. Ahmed, E.F. Nasir, J. Badra, G. Kalghatgi, S.M. Sarathy, H.J. Curran, A. Farooq, Autoignition characteristics of oxygenated gasolines, Combust. Flame 186 (2017) 114–128.
[45] H. El Merhubi, A. Kéromnès, G. Catalano, B. Lefort, L. Le Moyne, A high pressure experimental and numerical study of methane ignition, Fuel 177 (2016) 164–172, doi:10.1016/j.fuel.2016.03.016.
[46] E.L. Petersen, M.J.A. Rickard, M.W. Crofton, E.D. Abbey, M.J. Traum, D.M. Kalitan, A facility for gas- and condensed-phase measurements behind shock waves, Meas. Sci. Technol. 16 (2005) 1716–1729, doi:10.1088/0957-0233/16/9/003.
[47] D. Darcy, C.J. Tobin, K. Yasunaga, J.M. Simmie, J. Würmel, W.K. Metcalfe, T. Niass, S.S. Ahmed, C.K. Westbrook, H.J. Curran, A high pressure shock tube study of n-propylbenzene oxidation and its comparison with n-butylbenzene, Combust. Flame 159 (2012) 2219–2232, doi:10.1016/j.combustflame.2012.02.009.
[48] U. Burke, K.P. Somers, P. O'Toole, C.M. Zinner, N. Marquet, G. Bourque, E.L. Petersen, W.K. Metcalfe, Z. Serinyel, H.J. Curran, An ignition delay and kinetic modeling study of methane, dimethyl ether, and their mixtures at high pressures, Combust. Flame 162 (2015) 315–330, doi:10.1016/j.combustflame.2014.08.014.
[49] A. Kéromnès, W.K. Metcalfe, K.A. Heufer, N. Donohoe, A.K. Das, C.-J.J. Sung, J. Herzler, C. Naumann, P. Griebel, O. Mathieu, M.C. Krejci, E.L. Petersen, W.J. Pitz, H.J. Curran, An experimental and detailed chemical kinetic modeling study of hydrogen and syngas mixture oxidation at elevated pressures, Combust. Flame 160 (2013) 995–1011, doi:10.1016/j.combustflame.2013.01.001.
[50] R. Zellner, S.W. Benson, Thermochemical kinetics, 2nd ed., John Wiley & Sons, New York, London, Sydney, Toronto, 1976 320 Seiten, Preis: £ 16.-, $ 27.-, Berichte Der Bunsengesellschaft Für Phys. Chemie. 81 (1977) 877–878. doi:10.1002/bbpc.19770810919.
[51] E.R. Ritter, J.W. Bozzelli, THERM: thermodynamic property estimation for gas phase radicals and molecules, Int. J. Chem. Kinet. 23 (1991) 767–778, doi:10.1002/kin.550230903.

[52] C.-J. Sung, H.J. Curran, Using rapid compression machines for chemical kinetics studies, Prog. Energy Combust. Sci. 44 (2014) 1–18, doi:10.1016/j.pecs.2014.04.001.
[53] C.-W. Zhou, J.M. Simmie, H.J. Curran, Rate constants for hydrogen abstraction by HȮ2 from n-butanol, Int. J. Chem. Kinet. 44 (2012) 155–164, doi:10.1002/kin.20708.
[54] R. Sivaramakrishnan, M.-C. Su, J.V. Michael, S.J. Klippenstein, L.B. Harding, B. Ruscic, Rate constants for the thermal decomposition of ethanol and its bimolecular reactions with OH and D: reflected shock tube and theoretical studies, J. Phys. Chem. A 114 (2010) 9425–9439, doi:10.1021/jp104759d.
[55] I. Stranic, G.A. Pang, R.K. Hanson, D.M. Golden, C.T. Bowman, Shock tube measurements of the rate constant for the reaction ethanol + OH, J. Phys. Chem. A 118 (2014) 822–828, doi:10.1021/jp410853f.
[56] Z.F. Xu, K. Xu, M.C. Lin, Ab initio kinetics for decomposition/isomerization reactions of C_2H_5O radicals, ChemPhysChem 10 (2009) 972–982, doi:10.1002/cphc.200800719.
[57] J. Cai, W. Yuan, L. Ye, Z. Cheng, Y. Wang, L. Zhang, F. Zhang, Y. Li, F. Qi, Experimental and kinetic modeling study of 2-butanol pyrolysis and combustion, Combust. Flame 160 (2013) 1939–1957, doi:10.1016/J.COMBUSTFLAME.2013.04.010.
[58] E.E. Dames, Master equation modeling of the unimolecular decompositions of α-hydroxyethyl (CH_3CHOH) and ethoxy (CH_3CH_2O) radicals, Int. J. Chem. Kinet. 46 (2014) 176–188, doi:10.1002/kin.20844.
[59] F. Caralp, P. Devolder, C. Fittschen, N. Gomez, H. Hippler, R. Méreau, M.T. Rayez, F. Striebel, B. Viskolcz, The thermal unimolecular decomposition rate constants of ethoxy radicals, Phys. Chem. Chem. Phys. 1 (1999) 2935–2944, doi:10.1039/a901768b.
[60] H. Sun, J.W. Bozzelli, C.K. Law, Thermochemical and kinetic analysis on the reactions of O2 with products from OH addition to isobutene, 2-hydroxy-1,1-dimethylethyl, and 2-hydroxy-2-methylpropyl radicals: HO2 formation from oxidation of neopentane, part II, J. Phys. Chem. A 111 (23) (2007) 2974–4986, doi:10.1021/JP070072D.
[61] K.A. Sahetchian, R. Rigny, J. Tardieu de Maleissye, L. Batt, M. Anwar Khan, S. Mathews, The pyrolysis of organic hydroperoxides (ROOH), Symp. (Int.) Combust. 24 (1992) 637–643, doi:10.1016/S0082-0784(06)80078-0.
[62] S.L. Fischer, F.L. Dryer, H.J. Curran, The reaction kinetics of dimethyl ether. I: high-temperature pyrolysis and oxidation in flow reactors, Int. J. Chem. Kin. 32 (12) (2000) 713–740, doi:10.1002/1097-4601(2000)32:12⟨713::AID-KIN1⟩3.0.CO;2-9.
[63] H.J. Curran, S.L. Fischer, F.L. Dryer, C.E.T. Al, The reaction kinetics of dimethyl ether. II: low-temperature oxidation in flow reactors, Int. J. Chem. Kin. 32 (12) (2000) 741–759.
[64] Z. Zhao, M. Chaos, A. Kazakov, F.L. Dryer, Thermal decomposition reaction and a comprehensive kinetic model of dimethyl ether, Int. J. Chem. Kinet. 40 (2008) 1–18, doi:10.1002/kin.20285.
[65] Z. Li, W. Wang, Z. Huang, M.A. Oehlschlaeger, Dimethyl ether autoignition at engine-relevant conditions, Energy Fuels 27 (2013) 2811–2817, doi:10.1021/ef400293z.
[66] J. Li, A. Kazakov, M. Chaos, F.L. Dryer, Chemical kinetics of ethanol oxidation, 5th US Combustion Meeting, 2007.
[67] T.S. Norton, F.L. Dryer, An experimental and modeling study of ethanol oxidation kinetics in an atmospheric pressure flow reactor, Int. J. Chem. Kinet. 24 (1992) 319–344, doi:10.1002/kin.550240403.